Earthquake distribution and lithospheric rheology beneath the Northwestern Andes, Colombia

Carla Lagardère[1,2], Carlos A. Vargas[2]

1. Université de Bordeaux, Bordeaux, France
2. Department of Geosciences, Universidad Nacional de Colombia, Bogotá, Colombia

Carla Lagardère (clagardere@unal.edu.co)

Carlos A. Vargas (cavargasj@unal.edu.co)

Key Points

-We build a rheological model for the Northwestern Andes lithosphere using earthquake data.

-We hypothesise a delamination process occurring below the Eastern Cordillera of Colombia.

-The mechanical behaviour study of the lithosphere helps to understand geodynamical processes where two oceanic plates are converging against a continental plate.

Abstract

The rheological behavior of the lithosphere is examined beneath the Northwestern (NW) Andes (Colombian). Two profiles, one on western and other on eastern of the transition area between the Upper Magdalena Valley (UMV) and the Middle Magdalena Valley (MMV), are obtained from the analysis of the earthquake distribution and the stress drop. Results are consistent with the tectonic and geodynamic context of the western region. In essence, the brittle/ductile transition of the lithospheric crust and mantle is observed, and an approximation of the lithospheric thickness is made. Moreover, the subduction phenomenon of the Nazca Plate under the South American Plate is shown. In the Eastern region, we contemplate an aseismic zone under the Eastern Cordillera below 20 km deep that makes it challenging to know the crust/mantle boundary. This seismic particularity leads us to support the hypothesis of a delamination process due to the tectonic, geological, and thermal context. Our results suggest that the earthquake dataset correlated with rheological estimations may offer a consistent interpretation of the mechanical behavior of the lithosphere.

1. Introduction

Explain the mechanical behavior of the lithosphere has been essential to prove the brittle/ductile transition. Goetze and Evans (1979) were the first authors that proposed the first rheological profile to represent the mechanical behavior of the upper lithosphere. By computing the stress drop applied to the material as a function of depth, this profile allows us to study brittle and ductile deformations in the lithosphere, working with empirical laws. Much of the Earth's geological structures were formed and have evolved conforming to the mechanical behavior of the lithosphere (Burov, 2011). Watts and Burov (2003) have determined that this mechanical performance shows some correlation with short-time processes like seismicity, mostly in the crust. Indeed, the deep distribution of earthquakes is mainly controlled by the rheological properties of the upper lithosphere (Fernández-Ibáñez, 2005).

Many works have evidenced an intense seismic activity in NW Andes due to a complex geological context where the orogenic system growing up and expands horizontally with differential velocities from south to north, and that coexist with the convergence of three tectonic plates, South American, Nazca, and Caribbean Plates, in an active subduction setting (Adamek al., 1988; Tabaoda et al., 1998; Tabaoda et al., 2000; Ojeda and Havskov, 2001; Syracuse et al., 2016). In this region (Figure 1), the Central Cordillera (CC) was formed during the end of the Cretaceous (Butler and Schamel, 1988), probably related to the origin of the Nazca plate subduction (Taboada et al., 1998). Along this cordillera, a volcanic arc dating from the Eocene-Oligocene takes place (Butler and Schamel, 1988; Taboada et al., 1998). The Western Cordillera (WC) exhumation occurred because of the Nazca and the South American converging margin collided during the Cretaceous-Palaeocene interval (Taboada et al., 1998; Duque-Caro, 1990; Mora and al., 2006). The Eastern Cordillera (EC), the most recent, uplifted in the Miocene (Van der Hammen, 1958; Cooper al., 1995) after an inversion of a normal fault system (formed during the Jurassic) into a thrust fault system caused by the collision of the Panama Block with the Northwest of Colombia (Colletta al., 1990; Cooper et al., 1995; Mora et al., 2006).

In this work, we present two rheological profiles of the NW Andes based on a database of local earthquakes recorded by the Colombian National Seismological Network

(CNSN) between 1993 and 2019 (Figure 2a). Those events were used to determine the rock mechanical behavior under the orogenic system. Our profiles have been created computing the stress drop and using frictional and creep laws which may fit better our observational dataset. Taking into account those results, we propose a conceptual model of the lithospheric structure of the study area and we infer some geodynamical processes that are arising there. Figures 1 and 2 summarize the main morphotectonic features of the study region and show the location of the seismic stations belonging to the CNSN, which recorded the seismic events used in this paper.

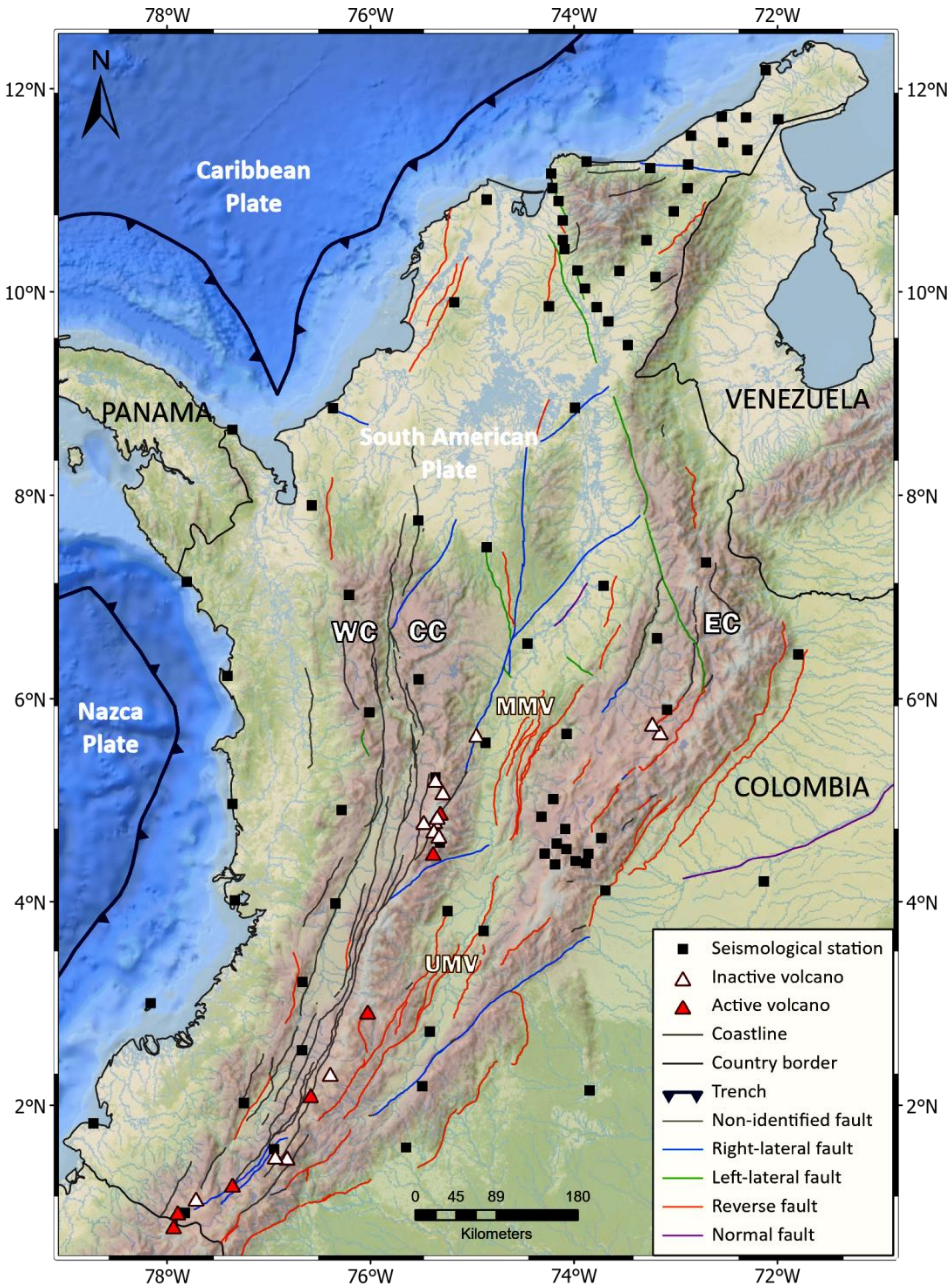

Figure 1. Tectonic map of Northwestern Andes with seismological stations of the CNSN and the main fault systems. EC: Eastern Cordillera, CC: Central Cordillera, WC: Western Cordillera, MMV = Middle Magdalena Valley, UMV = Upper Magdalena Valley. Bathymetry and topography from Ryan et al. (2009).

2. Data and Analysis

2.1. Earthquake dataset

Earthquakes used in this work have local magnitude (m_L) ranging between 3.5 and 6.7 and depths between 0 and 120 km. Figure 2b presents the projected areas on two profiles. Zone A, related to the western profile, includes 458 earthquakes, while zone B includes 243 earthquakes. The fault type, thrust or normal, associated to each earthquake have to be analyzed to separate the compressive and extensive stress dominant local fields for the rheological profiles. For this purpose, we used 25 focal mechanisms related to earthquakes with $m_L > 4$ (Figure 2b), which were reported by the Global Centroid Moment Tensor - CMT catalog solutions (Dziewonski et al., 1981; Ekström et al., 2012). The focal mechanism colors correspond to the depth of the earthquakes (Figure 2b). In Figures 2a and 2b, we have also included the Caldas Tear projection (Vargas and Mann, 2013), the volcano locations, and the seismic events reported by the CNSN to take into consideration the main tectonic features that may influence in the distribution of the earthquakes. We emphasize that the superficial compressive regime of the EC is the product of the Nazca Plate subduction and the Panama Arc floating block collision against the South America Plate (Vargas and Mann, 2013).

(a)

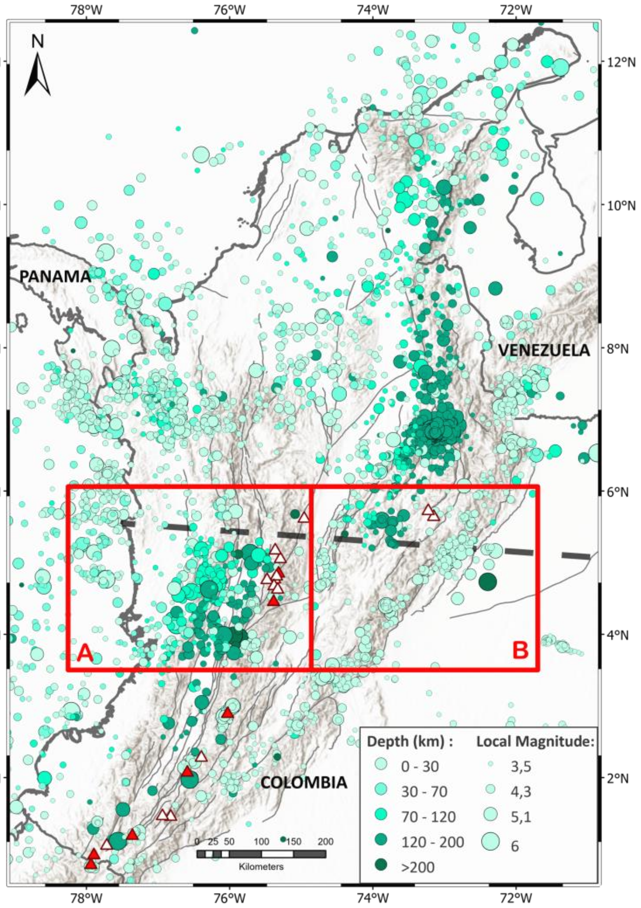

78ºW
76ºW
74ºW
72ºW
12ºN
10ºN
8ºN
6ºN
4ºN
2ºN
N
PANAMA
VENEZUELA
COLOMBIA
A
B
Depth (km) :
0 - 30
30 - 70
70 - 120
120 - 200
>200
Local Magnitude:
3,5
4,3
5,1
6
0 25 50 100 150 200
Kilometers

(b)

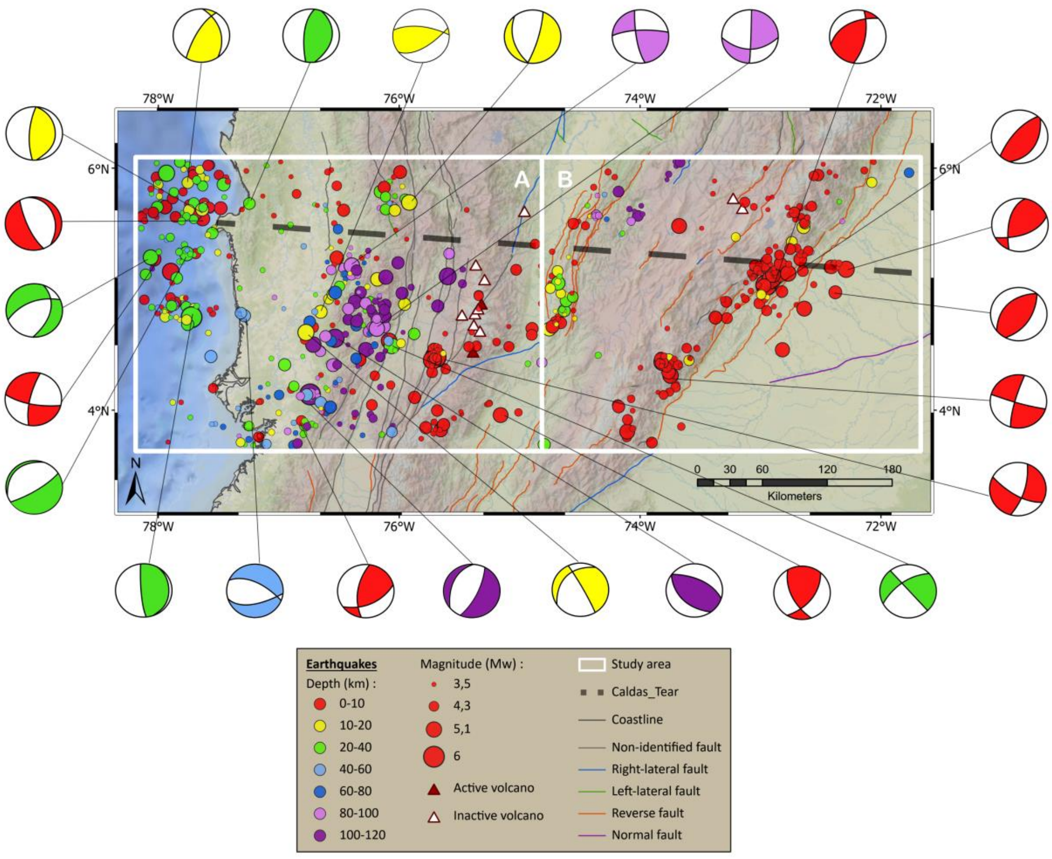

78ºW
76ºW
74ºW
72ºW
6ºN
4ºN
A
B
N
0 30 60 120 180
Kilometers
Earthquakes
Depth (km) :
0-10
10-20
20-40
40-60
60-80
80-100
100-120
Magnitude (Mw) :
3,5
4,3
5,1
6
Active volcano
Inactive volcano
Study area
Caldas_Tear
Coastline
Non-identified fault
Right-lateral fault
Left-lateral fault
Reverse fault
Normal fault

Figure 2. a) Seismicity in the NW Andes (from 3.5 to 6.7 mL) and location of the study area (red squares). b) Details of the study area with earthquake spatial distribution and the corresponding magnitude. Square A: Western area. Square B: Eastern area. Location of focal mechanisms used in this work (derived from CMT solutions, Dziewonski et al., 1981; Ekström et al., 2012) and their corresponding depths shown by colors. Red and white triangles represent active and inactive volcanoes, respectively, and the gray dashed line is the Caldas Tear.

2.2. Stress drop

To estimate the earthquake stress drop, we used the Eshelby's equation (1957):

$$\Delta\sigma = \frac{7M_0}{16r^3} \quad (1)$$

Where M_0 is the seismic moment, r is the radius of a circular fault. After that, Brune (1970) proposed an equation to find r value:

$$r = \frac{k\beta}{f_c} \quad (2)$$

Where k is a constant which depends on the theoretical model chosen, β is the shear-wave velocity, and f_c is the cut-off frequency. Thus, equation (1) becomes:

$$\Delta\sigma = \frac{7}{16}\left(\frac{f_c}{k\beta}\right)^3 M_0 \quad (3)$$

Following Madariaga (1977), we assume that $k = 0.32$ for P-waves and $v_r = 0.9\beta$, where v_r is the rupture velocity and corresponds in our work to the average of the S-wave velocity during its propagation. We determine β from the S-wave value at various depths provided by the IASP91 velocity model. In view of finding the cut-off frequency, we used waveforms from the CNSN and estimated f_c in the same way that Brune (1970) did with P-wave spectra and using linear regression. Due to the lack of data and inconvenience in the operation of some seismic stations, we assumed the f_c value for few earthquakes based on closeness to some analyzed earthquakes. We also converted local magnitudes m_L to moment magnitudes M_w to find the seismic moment M_0. Munafò et al. (2016) proposed the following equation for small earthquakes (m_L ranging between 3.5 and 4):

$$M_w = \frac{2}{3} * m_L + 1.15 \quad (4)$$

For more significant magnitude events, we adopt the Tang et al. (2016) formula:

$$M_w = 1.48 + 0.71 m_L \quad (5)$$

Therefore, we obtained M_0 employing Kanamori (1977) and Hanks and Kanamori (1979) works which establish that:

$$M_w = \frac{2}{3} * log10M_0 - 10.7 \quad \text{in dyn. cm} \quad (6)$$

$$M_w = \frac{2}{3} * log10M_0 - 6.07 \quad \text{in N. m} \quad (7)$$

2.3. Brittle behavior:

The deep seismicity contrast could be clarified by the brittle/ductile transition, constrained by the temperature that rules mainly the strength of the lithosphere (Parsons and Sclater, 1977; Meissner and Strehlau, 1982). The brittle deformation of the rocks means, in most cases, an intense seismic activity because of the weakness of the material, promoting a high cumulative stress drop. Ranalli (1995) describes the brittle failure with a linear law:

$$(\sigma 1 - \sigma 3) \geq \delta \rho g z (1 - \lambda) \quad (8)$$

Where $\sigma 1 - \sigma 3$ represents the differential stress, δ is a parameter which depends on the type fault associated with the earthquake, ρ is the material density ($\mathrm{kg.m^{-3}}$), g is the gravity acceleration on Earth, z is the depth, and λ is the pore fluid pressure. The upper crust, lower crust, and upper mantle densities are respectively 2750, 2950, and 3170 $\mathrm{kg.m^{-3}}$ (Solaro et al., 2007). We assumed a pore fluid factor of 0.4 for the Eastern region and 0.6 for the Western part supported in the near and far influence of the subduction process (Brace and Koldshedt, 1980). According to Ranalli (1995), for thrust faults $\delta = 3.0$, whereas $\delta = 0.75$ for normal faults. We have respected the limit condition of this law constraining differential stress values superior to the factor of these parameters.

2.4. Ductile behavior

While pressure and temperature increase, rocks adopt a ductile behavior leading to a diminution of the seismic activity (Scholz, 1990). The material deformation is constrained principally by dislocation mechanisms (Hull and Bacon, 1984). The cumulative stress drop decreases due to the lack of earthquakes, and the ductile behavior follows a non-linear law, the power-law creep (Kirby, 1983) :

$$\Delta\sigma = \left(\frac{\varepsilon}{A}\right)^{\left(\frac{1}{n}\right)} exp\left(\frac{Q}{nRT}\right) \quad (9)$$

Where ε is the strain rate (s^{-1}), A ($\mathrm{Pa.\,s}^{-1}$) and n are material parameters, Q is the activation energy ($\mathrm{kJ.\,mol}^{-1}$), R is the universal gas constant, and T is the temperature (°K). In this work, the strain rate is assumed as $10^{-14}\mathrm{s}^{-1}$.

2.5. Geothermal gradient

Temperature is a determining factor for the brittle and ductile behaviors of the lithosphere (Parsons and Sclater, 1977). Vargas et al. (2009) reported geothermal gradient estimations in Colombia derived from hydrocarbon wells observations (Figure 3). They suggested the presence of abnormally high geothermal gradients in the Eastern area (EC and the Eastern "Llanos"), whereas, in the Western region, the geothermal gradient is lower. Hence, we chose two different values of the geothermal gradient: $20°\mathrm{C/km}$ for zone A and $30°\mathrm{C/km}$ for zone B. We assumed an average temperature of the Earth's surface equal to $15°\mathrm{C}$.

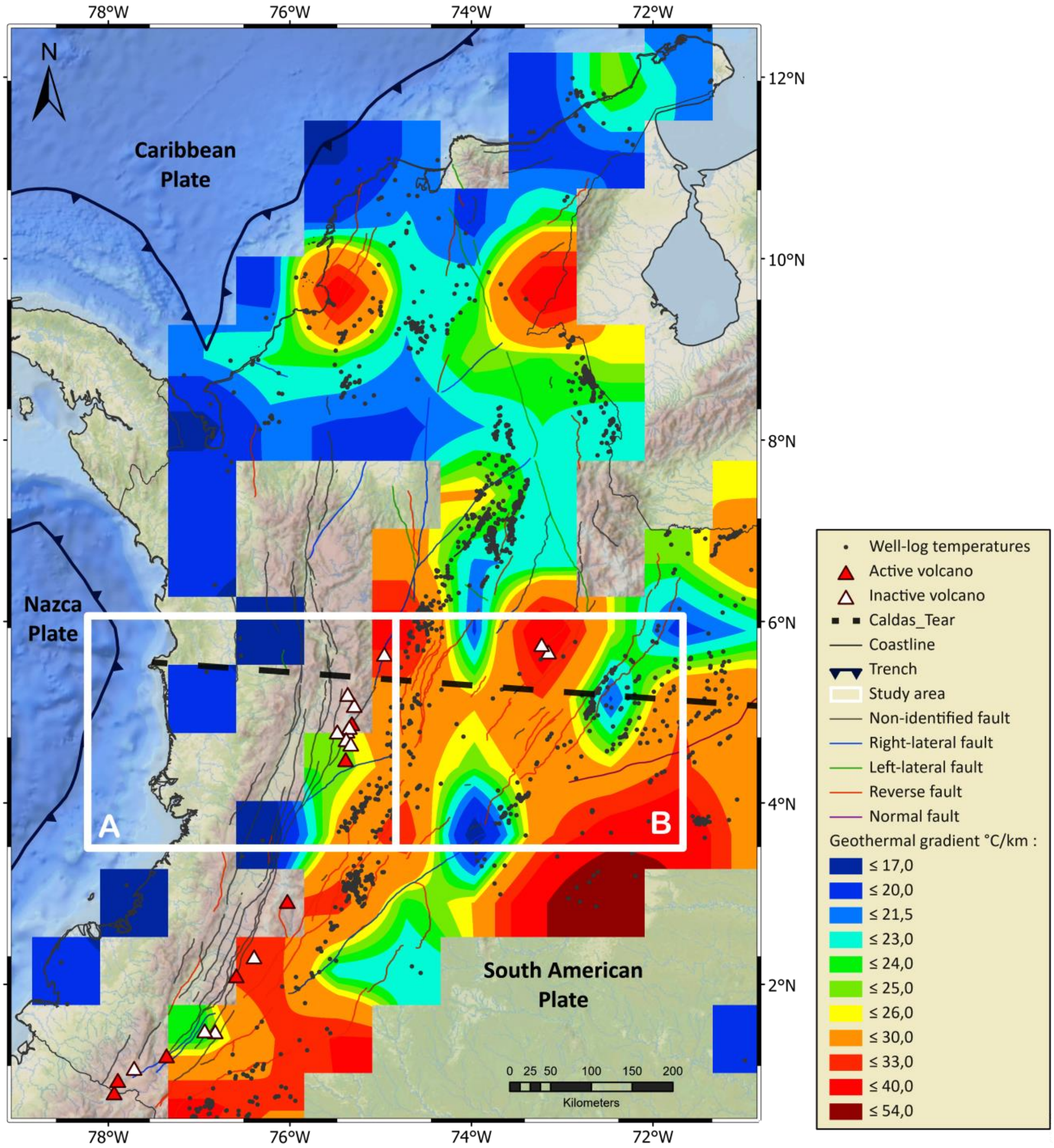

Figure 3. Geothermal gradient map of Colombia (geothermal measurements taken from Vargas et al., 2009). It includes faults, volcanoes (triangles), and the Caldas Tear (black dashed line). Few geothermal gradient observations are reported in the western study area. The eastern study area presents high geothermal gradient anomalies, mainly under the EC.

3. Results

The stress drop values obtained were ranging between 0.1 to 160 MPa for zone A and reached a maximum of 200 MPa for zone B with a mean value of $\sim 5.5\ \mathrm{MPa}$, which is closer to the results of Abercrombie et al. (2016), who obtained values among 1-100 MPa with an average of 10 MPa. Most elevated values correspond to high magnitude earthquakes. Nevertheless, small earthquakes (~ 3.5 to $4\ \mathrm{m_L}$) have a stress drop around 0.1 to 2 MPa, related to the cut-off frequencies estimated. Hence, we endeavored to fit brittle and creep laws with our experimental observations. For the creep law, we used A, n, and Q values, as are presented in Table 1.

Table 1. Creep laws parameters used and their references.

Material	$A\ (\mathrm{MPa^{-1}.s^{-1}})$	n	$Q\ (\mathrm{kJ.mol^{-1}})$	Reference
Dry Quartzite	3.2×10^{-5}	1.9	123	Lowry and Smith (1995)
Dry Granite	2.5×10^{-9}	3.4	139	Lowry and Smith (1995)
Wet Quartzite (upper crust)	2.91×10^{-3}	1.8	151	Behn et al. (2002)
Dry Quartzite (Intermediate Crust)	5×10^{-6}	3.2	220	Behn et al. (2002)
Wet Olivine	1.9×10^{5}	3.0	420	Karato et al. (1986)
Dunite	10^{4}	3.4	444	Chopra and Paterson (1981)
Wet Clinopyroxenite	$10^{5.7}$	3.3	490	Boland and Tullis (1986)

Previous results allowed us to establish two rheological profiles, the western one (Figure 4) and the eastern one (Figure 5). The brittle and ductile behaviors described by Ranalli (1995) and other authors listed in Table 1 are included in these profiles. We also indicate the brittle/ductile transition, as well as the boundary of each layer. For Zone A, we suggest the existence of an upper-crust, an intermediate crust, and a lithospheric mantle. At around 80 km deep, we observe a new increase of the stress drop. Creep laws defined by Lowry and Smith (1995) and Karato et al. (1986), fit better for the crust and the mantle, respectively. Figure 5 presents a very brittle upper crust and a thin intermediate crust barely visible. We focused on the first 60 km due to a negligible stress drop between 60 and 120 km. For zone B, creep laws described by Lowry and Smith (1995) and Behn et al. (2002) coincide well with our experimental observations.

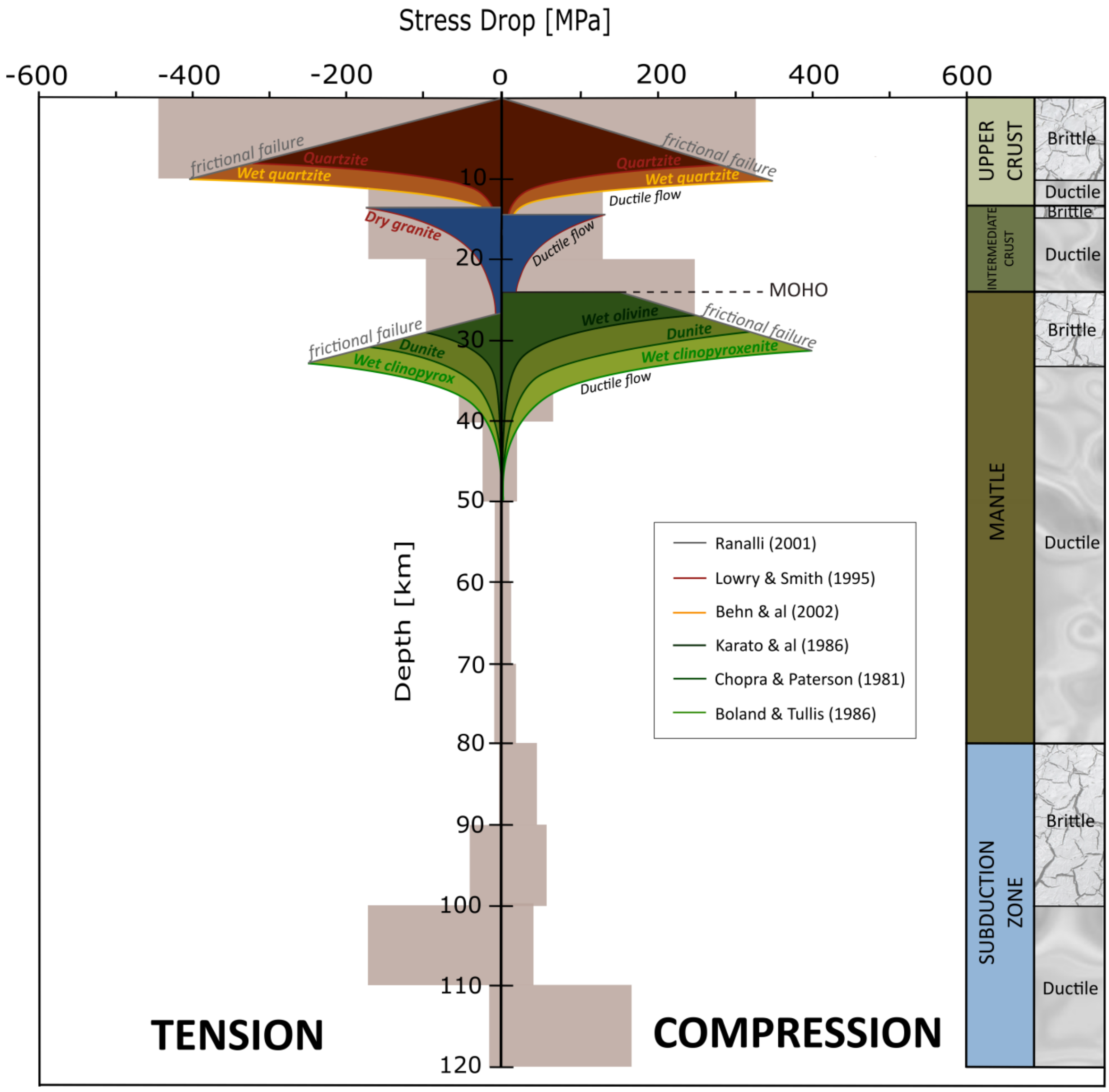

Figure 4. The western rheological profile shows the extensive regime at the left and the compressive regime at the right. Cumulative computed stress drops in [MPa] for each 10 km depth interval. Cumulative stress drops experimentally calculated are represented in light pink stripes. Frictional and creep laws are plotted with different lines of colors, according to the author. At the right of the profile, layers boundaries and brittle/ductile transitions are shown.

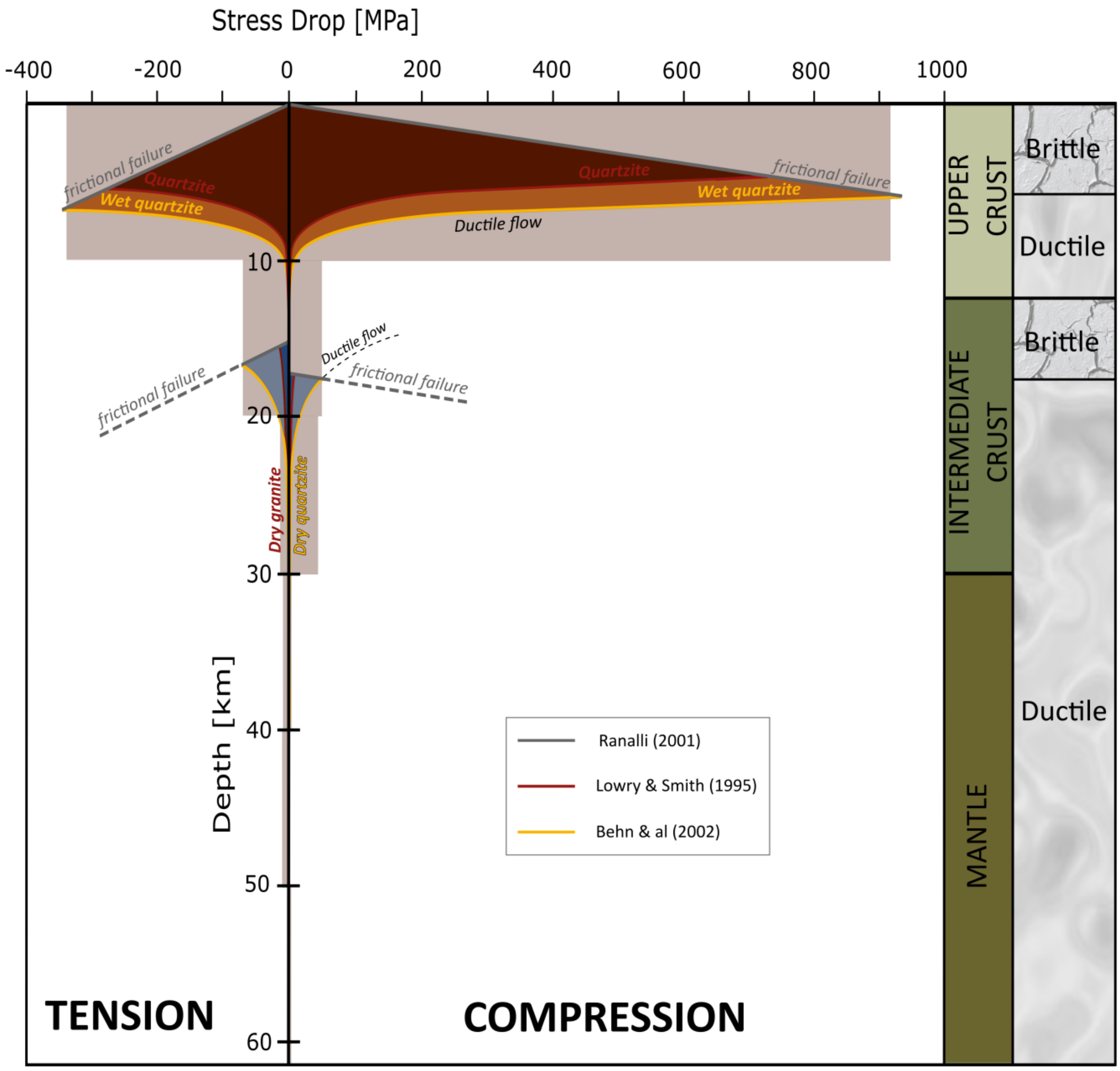

Figure 5. Eastern rheological profile shows the extensive regime at the left and the compressive regime at the right. Cumulative computed stress drops in [MPa] for each 10 km depth interval. Cumulative stress drops experimentally calculated are represented in light pink stripes. Frictional and creep laws are plotted with different lines of colors, according to the author. At the right of the profile, layers boundaries and brittle/ductile transitions are shown.

4. Discussion and Interpretation

4.1. Western Profile

The Western profile (Figure 4) suggests an upper-crust characterized by a high density of earthquakes at shallow depths, which reflect a brittle behavior. We interpret a thickness of the upper and intermediate crust of around 13 km and 10 km, respectively. The Mohorovicic discontinuity is located over 24 km deep beneath the coastal Pacific plains of Colombia, which is in agreement with the estimations of Poveda et al. (2015). This last author determined a crustal thickness of 35 km under the WC and approx. 50 km under the CC. The lithospheric mantle (LM) is less evident in the extensive regime than in the compressive one. We can explain this fact by the compressive motion, which intervenes at higher depths due to the subduction phenomenon between the Nazca and South American Plates that could also be the origin of the stress drop increment from 80 to 120 km (e.g., Andreescu and Demetrescu, 2001; Burov, 2011). According to Cloos et al. (2005), this lithospheric model could correspond to a thin continental transitional crust.

4.2. Eastern Profile

Figure 5 reveals a relevant contrast among the two regimes for the upper crust, where the compressive one predominates. With a thermal gradient larger than in the Western area, the upper crust is slightly thinner. However, we note the same brittle behavior as zone A. Intermediate crust is governed primarily by a ductile deformation, which could be justified by the low number of earthquakes recorded to more than 10 km away

(Scholz, 1990). Over 20 km deep, we observe almost an absence of seismic events; hence stress drop values only reach a few MPa. This profile does not indicate the Moho discontinuity, either the LM. Thus, we assume that beyond 17 km deep, the material has a ductile behavior, and we cannot determine the crust/mantle boundary. Nonetheless, Poveda et al. (2015) identified that below the EC, the crustal thickness might reach 60 km deep, which could coincide with a thick continental typical crust (Cloos and al., 2005). Bearing in mind the previous observations and the geological context, we do justify the non-conformity in the results between our work and that of Poveda et al. (2015), assuming a delamination phenomenon under the EC.

4.3. Cross-section

In furtherance of the rheological profile results, Figure 6 presents the distribution of the earthquakes in-depth with the associated topography and combines the two study areas. The cross-section F-F’ suggests firstly the Nazca subduction geometry in the western zone and secondly the presence of the Caribbean Plate subduction detectable below the EC (Taboada et al., 2000; Vargas and Mann, 2013). Also, it is shown that, for the eastern zone, earthquake distribution is mainly superficial and located under the foothill of the EC. The uncertainty in the depth values is sometimes not negligible, as we can see in this figure.

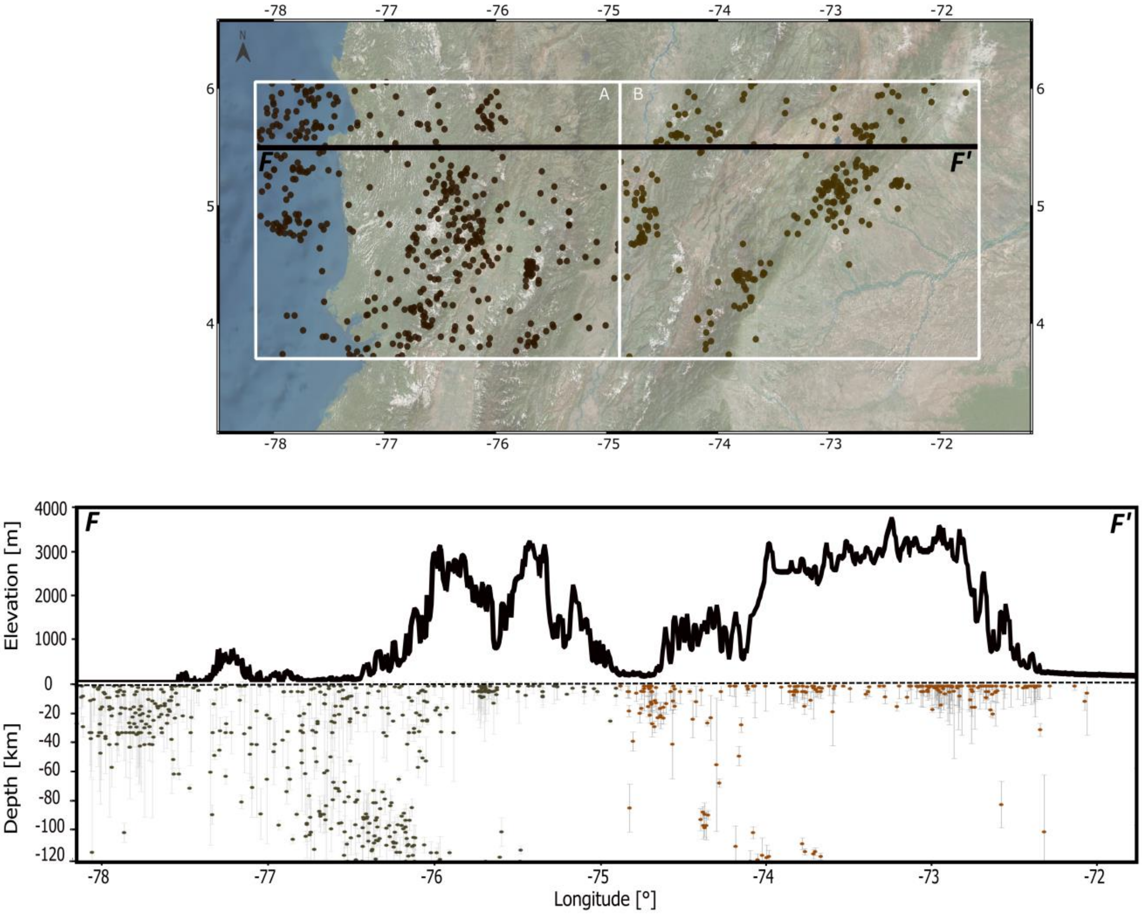

Figure 6. Cross-section of the all study area with hypocentre solutions. Transect F-F' shows the lateral changes of seismicity and topography of the entire area. Depth errors of hypocentre solutions are plotted in gray bars.

4.4. A rheological model of the NW Andes

Previous observations are summarized in the conceptual model (Figure 7). In this cross-section, we are representing the subduction geometry, seismicity, and topography of the entire study area. Eastern rheological profile (Figure 5) and cross-section F-F’ (Figure 6) evidenced strong shallow seismicity at the EC and an aseismic zone below 20 km deep. We interpreted this anomaly by formulating a delamination process hypothesis. Chicangana and Vargas (2008) have introduced this idea to justify the origin of the Bucaramanga nest at the west of the EC. Nevertheless, in the study area appears a possible shallow delamination process. We hypothesize that this process is a consequence of the Panama Arc collision against the South American Plate (Vargas and Mann, 2013), generating a fast uplift of the EC and the separation of the lower crust and the LM (Bird, 1978; Bird, 1979; Schott and Schmeling, 1998).

The LM, colder and denser than the asthenosphere, is under negatives buoyancy forces, which induce the decoupling crust/mantle, giving way to a vertical rise of the hot asthenosphere, and flowing along with rheological contrasts such as the Moho (Bird, 1978; Bird, 1979; Schott and Schmeling, 1998). Bird and Baumgardner (1981) suggested that the viscosity of the asthenosphere is a critical factor for the delamination process and has to be sufficiently high while the LM has a relatively low viscosity. In this scenario, the asthenosphere flows into fractures created by the dripping of the LM. Many works suggest that a thick lithosphere is necessary for this phenomenon, which is typically formed during compressive orogenies (Houseman et al., 1981; Platt and England, 1994; Schott and Shmeling, 1998). At the same time, delamination could be related to thinning and heating of the lower crust (Schott and Schmeling, 1998; Fillerup et al., 2010), that in our case may be associated with the Miocene – Present magmatic and hydrothermal activity in the EC (Pardo et al., 2005; Barrera et al., 2018).

In addition to the aseismic zone detected, the EC presents other features that allow us to assume a delamination process. Previous to the rising of the mountain range, the region was an extensive rifted sedimentary basin of Cretaceous age (Kellogg et al., 2005). This sedimentary basin was characterized by thick-skinned structural styles with deep faults (Chicangana et al., 2014). During the Miocene, the EC uplift occurred (Van der Hammen, 1958; Cooper et al., 1995) after a change from an extensive to a compressive regime by inversion of the faults due to the collision of the Panama Block with the North Andean Block (Colletta et al., 1990; Cooper et al., 1995; Taboada et al., 2000; Kellogg et al., 2005; Mora et al., 2006). This tectonic inversion caused weak zones in the continental crust and the apparition of the thin-skinned structural styles (e.g., Dengo and Covey, 1993). After the uplifting and the shortening associated (140 - 150 km, according to Kellogg et al., 2005), the crust thickened, forming a deeper crustal root. Poveda et al. (2015) described a crustal thickness higher than 50 km. In this context, we have to take into account the presence of the Caldas Tear (Vargas and Mann, 2013), an east–west-striking tear-slab, which is splitting zone B into two parts. In Figure 3, we also observe abnormally high thermal gradients at the North of the Caldas Tear. This anomaly can be related to the existence of magma, and hydrothermal fluid flows, which are visible at the surface along a broad thermal springs field near to the Paipa–Iza volcanic complex, currently inactive. According to Poveda et al. (2015), the North part of zone B is slightly less thick than the South region, where geothermal anomalies are lower. The delamination could cause a shallowing of the asthenosphere along the base of the crust, generating magmatic activity and geothermal anomalies affecting the lithosphere at least from 30-50 km from the surface. Following this reasoning, the LM could be located at around 50-60 km deep, as Poveda et al. (2015) suggest. This argument could explain the impossibility with our results to determine the Moho depth while Poveda et al. (2015) have succeeded identified it. The compressive system of the EC with weak zones in the crust, the high geothermal gradients in this zone, the thin lower crust, the pre-Quaternary volcanic activity, and the thermal springs fields at the surface are additional evidence to assume a delamination process below the EC.

Conclusions of Seber (1996) about the Alboran Sea are relatively similar to ours, with a tectonic inversion earlier to a possible delamination of the LM and thinning of the crust argued by an aseismic zone in the depth range from 20 to 60 km. Fillerup et al. (2010) hypothesized a change in the location of the lower crust due to delamination, which could be represented by the Vancrea seismogenic zone.

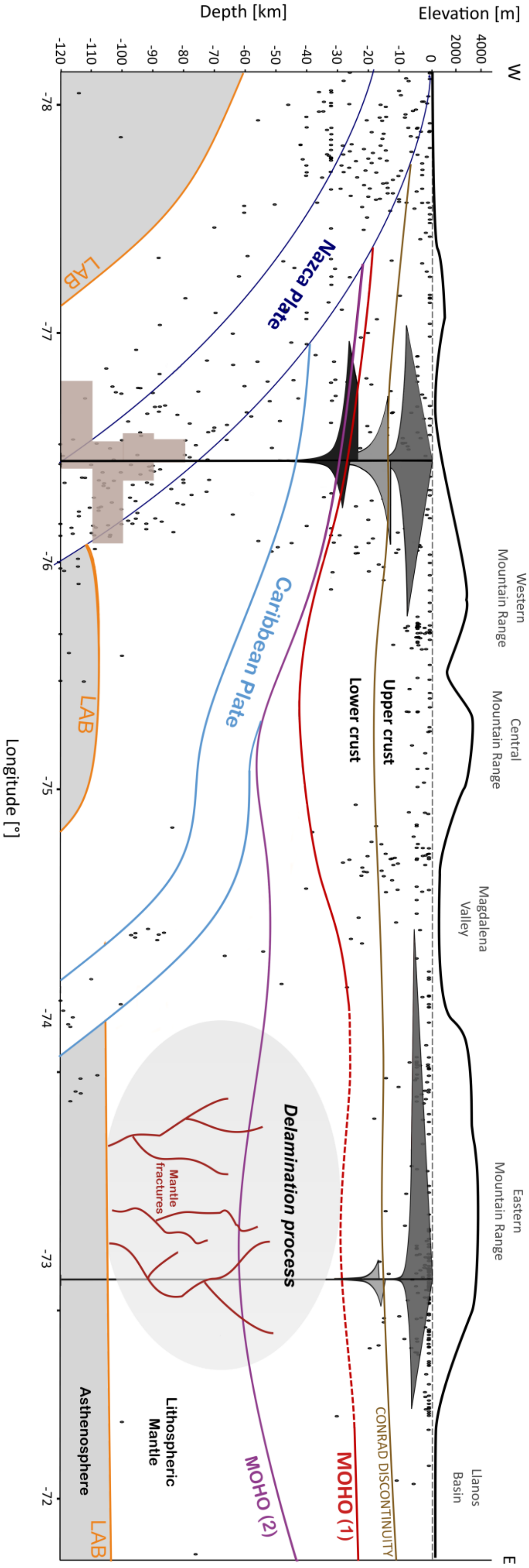

W
E
Elevation [m]
Depth [km]
Western Mountain Range
Central Mountain Range
Magdalena Valley
Eastern Mountain Range
Llanos Basin
Nazca Plate
Caribbean Plate
Upper crust
Lower crust
Delamination process
Mantle fractures
Lithospheric Mantle
Asthenosphere
CONRAD DISCONTINUITY
MOHO (1)
MOHO (2)
LAB
LAB
LAB
Longitude [°]

Figure 7. Conceptual model representing our results and interpretations. The elevation profile is presented with a black thick line. Earthquakes are plotted with brown points. The two rheological profiles are joined. The Conrad discontinuity is shown with a yellow line separating the upper crust from the lower crust. The experimental MOHO discontinuity (1) is the red line between the lower crust and the upper mantle. The dotted section means the uncertainty of the Moho location. The MOHO (2), with a purple line, corresponds to the results obtained by Poveda et al. (2015). The orange line is the lithosphere-asthenosphere boundary (LAB) with values obtained by Blanco et al. (2017). Subduction processes are charted, considering the earthquake distribution and rheological profiles. The delamination process is suggested with a gray circular polygon.

The relation between the long-term ductile strength of the lithosphere and the earthquake is not clear, as is reported by some authors (e.g., Handy and Brun, 2004; Burov, 2011). Hence, Burov (2011) pointed out that the time scale in terms of seismicity is much shorter than the rheological one, which makes difficult a correlation between seismological and rheological behavior. Future works in this region shall consider a more detailed thermal structure in depth, evaluation of rock chemical composition, and incorporating accurate gravity, density, and viscosity assessment. We propose this conceptual model (Figure 7) as the interpretation of our results. Nevertheless, there are significant uncertainties to take into account related to the depth of the earthquakes, and the absence of data in some parameters. This study is based on the use of seismic data for establishing a possible rheological and geodynamical explanation of the area by following similar strategies used in other works (e.g., Déverchère and al., 2001; Fernández-Ibañez and al., 2005; Solaro and al., 2007; Yang and Chen, 2010).

5. Conclusion

Through a database of earthquakes collected by the CNSN, we estimated a rheological model of the NW Andes by incorporating the stress drop for several seismic events, thermal structure, stress regime, and some reported mechanical properties of the lithospheric system. We fitted brittle and creep laws to our experimental results, and inferred lateral variations of the tectonic regime due to the subduction of the Nazca and Caribbean oceanic plates under the South American continental plate. We also found that those oceanic plates introduce significant rheological and geothermal anomalies beneath de EC, leading us to hypothesize a delamination phenomenon that could affect almost 40 km of the shallow lithosphere thickness. This process promotes an upward of the asthenosphere and thinning of the crustal thickness. We propose a conceptual model trying to incorporate diverse geophysical observations reported to make a geodynamic and mechanical interpretation of the study area. This paper is a first approach to provide a global rheological model of the Northwestern Andes, and it expects a future refinement based on new pieces of evidence that improve the understanding of the observed anomalies.

Acknowledgments

We are very grateful to the Geophysical Research Group belonging to the Geosciences Department of the Universidad Nacional de Colombia at Bogota. We also thank the Colombian National Seismological Network and the Global Centroid Moment Tensor for providing the datasets used in this study, available on https://www2.sgc.gov.co/sgc/sismos/Paginas/catalogo-sismico.aspx and https://www.globalcmt.org/CMTsearch.html. The support of Nicolás Pinzón Matapí brought useful advice for the realization of this work. This work was done without funding.

References

Abercrombie, R. E., Bannister, S., Ristau, J., and Doser, D. (2016). Variability of earthquake stress drop in a subduction setting, the Hikurangi Margin, New Zealand. *Geophysical Journal International, 208(1),* 306–320.

Adamek, S., Frohlich, C., and Pennington, W. D. (1988). Seismicity of the Caribbean-Nazca Boundary: Constraints on microplate tectonics of the Panama region. *Journal of Geophysical Research, 93(B3),* 2053-2075.

Andreescu, M., and Demetrescu, C. (2001). Rheological implications of the thermal structure of the lithosphere in the convergence zone of the Eastern Carpathians. *Journal of Geodynamics, 31(4),* 373–391.

Barrera, C. A., Vargas, C. A., and Cortes, J.E. (2018). Establishing geothermometric constraints on the local geothermal gradients: Case study of the Eastern Cordillera Basin, Colombia. *Geodesy and Geodynamics, 9(4),* 271-280.

Behn, M. D., Lin, J., and Zuber, M. T. (2002). A continuum mechanics model for normal faulting using a strain-rate softening rheology: implications for thermal and rheological controls on continental and oceanic rifting. *Earth and Planetary Science Letters, 202(3-4)*, 725–740.

Bird, P. (1978). Initiation of intracontinental subduction in the Himalaya. *Journal of Geophysical Research: Solid Earth, 83(B10),* 4975–4987.

Bird, P. (1979). Continental delamination and the Colorado Plateau. *Journal of Geophysical Research: Solid Earth, 84(B13),* 7561–7571.

Bird, P., and Baumgardner, J. (1981). Steady propagation of delamination events. *Journal of Geophysical Research: Solid Earth, 86(B6),* 4891–4903.

Blanco, J. F., Vargas, C. A., and Monsalve, G. (2017). Lithospheric thickness estimation beneath Northwestern South America from an S -wave receiver function analysis. *Geochemistry, Geophysics, Geosystems, 18(4),* 1376–1387.

Boland, J. N., and Tullis, T. E. (1986). Deformation behavior of wet and dry clinopyroxenite in the brittle to ductile transition region. *Geophysical Monograph Series,* 35–49.

Brace, W. F., and Kohlstedt, D. L. (1980). Limits on lithospheric stress imposed by laboratory experiments. *Journal of Geophysical Research: Solid Earth, 85(B11),* 6248–6252.

Brune, J. N. (1970). Tectonic stress and the spectra of seismic shear waves from earthquakes. *Journal of Geophysical Research, 75(26),* 4997–5009.

Burov, E. B. (2011). Rheology and strength of the lithosphere. *Marine and Petroleum Geology, 28(8),* 1402–1443.

Butler, K., and Schamel, S. (1988). Structure along the eastern margin of the central Cordillera, upper Magdalena Valley, Colombia. *Journal of South American Earth Sciences, 1(1),* 109–120.

Chicangana, G., and Vargas, C. A. (2008). Seismotectonic analysis of the Bucaramanga Seismic Nest, Colombia. *7th International Symposium on Andean Geodynamics (ISAG 2008, Nice),* Extended Abstracts: 128-131.

Chicangana, G., Vargas, C. A., Caneva, A., Salcedo Hurtado, E., Gómez Capera, A. (2014). La amenaza sísmica de la Sabana de Bogotá frente a un sismo de magnitud M>7.0, cuyo origen esté en el Piedemonte Llanero. *Cuadernos de Geografía, Revista Colombiana de Geografía, 24(2),* 73-91.

Chopra, P. N., and Paterson, M. S. (1981). The experimental deformation of dunite. *Tectonophysics, 78(1-4),* 453–473.

Cloos, M., Sapiie, B., Quarles van Ufford, A., Weiland, R. J., Warren, P. Q., and McMahon, T. P. (2005). Collisional delamination in New Guinea: The geotectonics of subducting slab breakoff. *Geological Society of America, Special Paper 400,* 1-51.

Colletta, B., Hebrard, F., Letouzey, J., Werner, P., and Rudkiweicz, J. L. (1990). Tectonic style and crustal structure of the Eastern Cordillera, Colombia from a balanced cross section. *Petroleum and Tectonics in Mobile Belts, edited by J. Letouzey, Editions Technip, Paris*, 81-100.

Cooper, M. A., Addison, F. T., Álvarez, R., Coral, M., Graham, R. H., Hayward, S. H., Martínez, J., Naar, J., Peñas, R., Pulham, A. J., and Taborda, A. (1995). Basin development and tectonic history of the Llanos Basin, Eastern Cordillera, and Middle Magdalena Valley, Colombia. *American Association of Petroleum Geologists Bulletin, 79 (10),* 1421-1443.

Dengo, C., and Covey, M. (1993). Structure of the Eastern Cordillera of Colombia: implications for trap styles and regional tectonics. *Bulletin of the Seismological Society of America, 77(8),* 1315-1337.

Déverchère, J., Petit, C., Gileva, N., Radziminovitch, N., Melnikova, V., and San'Kov, V. (2001). Depth distribution of earthquakes in the Baikal rift system and its implications for the rheology of the lithosphere. *Geophysical Journal International, 146(3),* 714–73.

Duque-Caro, H. (1990). The Choco Block in the northwestern corner of South America: Structural, tectonostratigraphic and paleogeographic implications. *Journal of South American Earth Sciences, 3,* 71-84.

Dziewonski, A. M., Chou T.-A., and Woodhouse, J. H. (1981). Determination of earthquake source parameters from waveform data for studies of global and regional seismicity. *Journal of Geophysical Research, 86,* 2825-2852.

Ekström, G., Nettles, M., and Dziewonski, A. M. (2012). The global CMT project 2004-2010: Centroid-moment tensors for 13,017 earthquakes. *Physics of the Earth and Planetary Interiors, 200-201,* 1-9.

Eshelby, J. D. (1957). The determination of the elastic field of an ellipsoidal inclusion, and related problems. *Proceedings of the Royal Society A: Mathematical, Physical and Engineering Sciences, 241(1226),* 376–396.

Fernández-Ibáñez, F., Soto, J. I., and Morales, J. (2005). Profundidad de la transición dúctil-frágil en la corteza de Béticas-Rif y Mar de Alborán. *Geogaceta, 37,* 155-158.

Fillerup, M. A., Knapp, J. H., Knapp, C. C., and Raileanu, V. (2010). Mantle earthquakes in the absence of subduction? Continental delamination in the Romanian Carpathians*. Lithosphere, 2(5),* 333–340.

Goetze, C., and Evans, B. (1979). Stress and temperature in the bending lithosphere as constrained by experimental rock mechanics. *Geophysical Journal International, 59(3),* 463–478.

Handy, M., and Brun, J.-P. (2004). Seismicity, structure and strength of the continental lithosphere. *Earth and Planetary Science Letters, 223(3-4),* 427–441.

Hanks, T. C., and Kanamori, H. (1979). A moment magnitude scale. *Journal of Geophysical Research, 84(B5),* 2348-2350.

Houseman, G. A., McKenzie, D. P., and Molnar, P. (1981). Convective instability of a thickened boundary layer and its relevance for the thermal evolution of continental convergent belts. *Journal of Geophysical Research: Solid Earth, 86(B7),* 6115–6132.

Kanamori, H. (1977). The energy release in great earthquakes. *Journal of Geophysical Research, 82(20),* 2981–2987.

Karato, S.-I., Paterson, M. S., and FitzGerald, J. D. (1986). Rheology of synthetic olivine aggregates: Influence of the grain size and water. *Journal of Geophysical Research, 91(B8),* 8151-8176.

Kellogg, J., Ojeda, G., Duque, H., and Ceron, J. (2005). Crustal structure of the Eastern Cordillera, Colombia. *6^{th} International Symposium on Andean Geodynamics, Barcelona,* Extented Abstracts: 424-427.

Kirby, S. H. (1983). Rheology of the lithosphere. *Reviews of Geophysics and Space Physics, 21,* 1458–1487.

Lowry, A. R., and Smith, R. B. (1995). Strength and rheology of the western U.S. Cordillera. *Journal of Geophysical Research: Solid Earth, 100(B9),* 17947–17963.

Madariaga, R. (1976). Dynamics of an expanding circular fault. *Bulletin of the Seismological Society of America, 66(3),* 639–666.

Meissner, R., and Strehlau, J. (1982). Limits of stresses in continental crusts and their relation to the depth-frequency distribution of shallow earthquakes. *Tectonics, 1(1),* 73–89. doi:

Mora, A., Parra, M., Strecker, M. R., Kammer, A., Dimaté, C., and Rodríguez, F. (2006). Cenozoic contractional reactivation of Mesozoic extensional structures in the Eastern Cordillera of Colombia. *Tectonics, 25(2),* 1-19.

Munafò, I., Malagnini, L., and Chiaraluce, L. (2016). On the Relationship between Mw and ML for Small Earthquakes. *Bulletin of the Seismological Society of America, 106(5),* 2402–2408.

Ojeda, A., and Havskov, J. (2001). Crustal structure and local seismicity in Colombia. *Journal of Seismology, 5(4),* 575–593.

Parsons, B., and Sclater, J. G. (1977). An analysis of the variation of ocean floor bathymetry and heat flow with age. *Journal of Geophysical Research, 82(5),* 803–827.

Pardo, N., Jaramillo, J. M., and Cepeda, H. (2005). The Paipa Volcano, Eastern Cordillera of Colombia, South America (Part II): Petrography and major elements petrology. *Earth Sciences Reasearch Journal, 9(2),* 148-164.

Platt, J. P., and England, P. C. (1994). Convective removal of lithosphere beneath mountain belts; thermal and mechanical consequences. *American Journal of Science, 294(3),* 307–336.

Poveda, E., Monsalve, G., and Vargas, C. A. (2015). Receiver functions and crustal structure of the northwestern Andean region, Colombia. *Journal of Geophysical Research: Solid Earth, 120(4),* 2408–2425.

Ranalli, G. (1995). Rheology of the Earth. *2nd edition Chapman and Hall, London*, 412 p.

Ryan, W. B. F., Carbotte, S. M., Coplan, J., O'Hara, S., Melkonian, A., Arko, R., Weissel, R. A., Ferrini, V., Goodwillie, A., Nitsche, F., Bonczkowski, J., and Zemsky, R. (2009). Global Multi-Resolution Topography (GMRT) synthesis data set. *Geochemistry, Geophysics, Geosystems, 10,* Q03014.

Scholz, C. H. (1990). The Mechanics of Earthquake and Faulting. *Cambridge University Press, Cambridge,* 512 p.

Schott, B., and Schmeling, H. (1998). Delamination and detachment of a lithospheric root. *Tectonophysics, 296(3-4),* 225–247.

Seber, D., Barazangi, M., Ibenbrahim, A., and Demnati, A. (1996). Geophysical evidence for lithospheric delamination beneath the Alboran Sea and Rif–Betic mountains. *Nature, 379(6568),* 785–790.

Solaro, G., Tizzani, P., Milano, G., and Pauselli, C. (2007). Rheological behaviour of the crust in Southern Apennine (Italy): results from a thermal and seismological study. *Terra Nova, 19(5),* 353–359.

Syracuse, E. M., Maceira, M., Prieto, G. A., Zhang, H., and Ammon, C. J. (2016). Multiple plates subducting beneath Colombia, as illuminated by seismicity and velocity from the joint inversion of seismic and gravity data. *Earth and Planetary Science Letters, 444,* 139–149.

Taboada, A., Dimaté, C., and Fuenzalida, A. (1998). Sismotectónica de Colombia: deformación continental activa y subducción. *Física de la Tierra, 10,* 111-147.

Taboada, A., Rivera, L. A., Fuenzalida, A., Cisternas, A., Philip, H., Bijwaard, H., Olaya, J., and Rivera, C. (2000). Geodynamics of the Northern Andes, subductions and intracontinental deformation (Colombia). *Tectonics, 19(5),* 787–81.

Tang, C., Zhu, L., and Huang, R. (2016). Empirical Mw–ML, mb, and Ms Conversions in Western China. *Bulletin of the Seismological Society of America, 106(6),* 2614–2623.

Van der Hammen, T. (1958). Estratigrafía del Terciario y Maestrichtiano Continentales y tectogénesis de los Andes Colombianos. *Boletín Geológico, Ingeominas, Bogotá, 6(1-3),* 67-128.

Vargas, C. A., Alfaro, C., Briceño, L. A., Alvarado, I., and Quintero, W. (2009). Mapa Geotérmico de Colombia. *Proceedings of X Simposio Bolivariano Exploración Petrolera en Cuencas Subandinas, Colombia (in Spanish).*

Vargas, C. A., and Mann, P. (2013). Tearing and breaking off of subducted slabs as the result of collision of the Panama arc-indenter with Northwestern South America. *Bulletin of the Seismological Society of America, 103(3),* 2025–2046.

Watts, A. B., and Burov, E. (2003). Lithospheric strength and its relationship to the elastic and seismogenic layer thickness. *Earth and Planetary Science Letters, 213(1-2),* 113–131.

Yang, Z., and Chen, W.-P. (2010). Earthquakes along the East African Rift System: A multiscale, system-wide perspective. *Journal of Geophysical Research, 115(B12).*